



ELSEVIER

Contents lists available at SciVerse ScienceDirect

Journal of Luminescence

journal homepage: www.elsevier.com/locate/jlumin

Ground- and excited-state absorption and emission spectroscopy of Nd:GGG

R. Soulard, B. Xu, J.L. Doualan, P. Camy, R. Moncorgé*

Centre de recherche sur les Ions, les Matériaux et la Photonique (CIMAP), UMR 6252 CEA-CNRS-ENSICAEN, Université de Caen Basse-Normandie, 6 Boulevard Maréchal Juin, 14050 Caen, France

ARTICLE INFO

Article history:

Received 10 January 2012

Received in revised form

8 March 2012

Accepted 26 March 2012

Available online 3 April 2012

Keywords:

Luminescence

ESA

Cr

GGG

Laser material

ABSTRACT

Complete room temperature absorption, excited-state absorption and emission spectra of Nd:GGG have been registered and calibrated in cross section units in the near infrared around the main pump and laser emission transitions of Nd:GGG.

© 2012 Elsevier B.V. All rights reserved.

1. Introduction

Among other neodymium-doped materials, Gadolinium Gallium Garnet, Nd:GGG, has a number of advantages like the possibility to be grown in larger size [1], a good thermal capacity of 0.38 J/(g K) [2] and a weak concentration quenching offering the possibly of higher doping levels, around 4% in contrast to about 1.5% in the case of YAG [3,4]. Moreover, Nd:GGG is characterized by two emission lines at 933.6 and 937.3 nm which could lead, after frequency-doubling, to two laser emissions at 466.8 and 468.6 nm, instead of 938.5/2=469.2 nm and 946/2=473 nm in the case of Nd:YAG. In fact, 468.8 nm is a wavelength which better fits with an absorption line of the Pr:YLF laser system which is presently investigated by several groups for the RGB laser application [5–7]. A compact and powerful diode-pumped and frequency doubled Nd:GGG laser thus would be an interesting alternative to the other pump sources provided by the GaN laser diodes and the frequency-doubled OPSLs which have been used so far around 445 nm and 477 nm for that application.

We focused here in this work on a detailed spectroscopic analysis of Nd:GGG. Indeed, the data which can be found in the past literature both contains some uncertainties, and need to be completed to be really useful for solid-state laser physicists. In particular, complete emission spectra are reported for the first time and they are calibrated in cross section unit by using experimentally derived

branching ratios instead of branching ratios calculated from a Judd–Ofelt analysis of the absorption spectra.

2. Literature data

The first spectral data were reported by Geusic et al. [8] but only around 1.06 μm and the first analysis of the luminescence properties of Nd:GGG was reported by Krupke [9] without showing, however, any absorption or emission spectra. He measured and calculated the strengths of the main absorption lines; then he performed the Judd–Ofelt (J.O.) analysis to derive the following J.O. parameters and branching ratios:

$$\Omega_2 = 0, \quad \Omega_4 = 3.3 \times 10^{-20} \text{ cm}^2, \quad \Omega_6 = 3.7 \times 10^{-20} \text{ cm}^2,$$

$$\begin{aligned} \beta(^4F_{3/2} \rightarrow ^4I_{9/2}) &= 35\%, & \beta(^4F_{3/2} \rightarrow ^4I_{11/2}) \\ &= 54\%, & \beta(^4F_{3/2} \rightarrow ^4I_{13/2}) \\ &= 11\% & \text{and } \beta(^4F_{3/2} \rightarrow ^4I_{15/2}) = 0.003 \end{aligned}$$

Using the β value thus found for the $^4F_{3/2} \rightarrow ^4I_{11/2}$ transition and the line-shape for the 1.0622 μm emission line, as reported by Geusic et al., the stimulated emission $\sigma_{em}(1.0622 \mu\text{m}) = 4.3 \times 10^{-19} \text{ cm}^2$ was derived, if the 44 cm⁻¹ splitting of the emitting level $^4F_{3/2}$ is taken into account, or $\sigma_{em}(1.0622 \mu\text{m}) = 1.92 \times 10^{-19} \text{ cm}^2$, if it is not. It is to be compared, for instance, with the values of 8.4 × 10⁻¹⁹ cm² and 3.3 × 10⁻¹⁹ cm² which can be found for the 1.064 μm laser line of Nd:YAG if the splitting of 88 cm⁻¹ of the $^4F_{3/2}$ emitting level is or is not taken into account.

These J.O. parameters were established by assuming a dopant concentration of 0.58 Nd at%, thus 0.73 × 10²⁰ ions/cm³ and by

* Corresponding author. Tel.: +33 231 452558; fax: +33 231 452557.
E-mail address: richard.moncorge@ensicaen.fr (R. Moncorgé).

equating the calculated radiative lifetime with the measured fluorescence lifetime extrapolated at zero concentration, i.e. $\tau_f=250 \mu\text{s}$ (which assumes no multiphonon relaxation).

The detailed positions of the Stark components of each energy level were reported by Kaminskii et al. [10] and Kaminskii [11]. The authors also reported the $1.0622 \mu\text{m}$ emission cross section $\sigma_{em}(1.0622 \mu\text{m})=2.9 \times 10^{-19} \text{cm}^2$. Finally, Lomheim and De Shazer [12] revisited the strengths of the absorption lines, again without showing any spectra. Based on the new set of J.O. parameters

$$\Omega_2 = 0.05 \times 10^{-20} \text{cm}^2, \quad \Omega_4 = 3.25 \times 10^{-20} \text{cm}^2, \quad \Omega_6 = 3.66 \times 10^{-20} \text{cm}^2$$

and the radiative lifetime $\tau=250 \mu\text{s}$, they derived the following branching ratios:

$$\begin{aligned} \beta(^4F_{3/2} \rightarrow ^4I_{9/2}) &= 43.5\%, \quad \beta(^4F_{3/2} \rightarrow ^4I_{11/2}) \\ &= 45.5\%, \quad \beta(^4F_{3/2} \rightarrow ^4I_{13/2}) = 10.7\% \end{aligned}$$

and

$$\beta(^4F_{3/2} \rightarrow ^4I_{15/2}) = 0.003$$

which is substantially different, especially for the transitions around 880 nm ($^4F_{3/2} \rightarrow ^4I_{9/2}$ transition) and $1.06 \mu\text{m}$ ($^4F_{3/2} \rightarrow ^4I_{11/2}$ transition), from Krupke's results.

The same analysis for Nd:YAG gave

$$\begin{aligned} \beta(^4F_{3/2} \rightarrow ^4I_{9/2}) &= 37\%, \quad \beta(^4F_{3/2} \rightarrow ^4I_{11/2}) \\ &= 50\%, \quad \beta(^4F_{3/2} \rightarrow ^4I_{13/2}) = 13\% \end{aligned}$$

and

$$\beta(^4F_{3/2} \rightarrow ^4I_{15/2}) = 0.003$$

It is also worth noting that the laser gain measurements performed by Rotter and Dane [13] who derived (by using a lifetime of $26.5 \mu\text{s}$) the $1.0622 \mu\text{m}$ emission cross section $\sigma_{em}(1.0622 \mu\text{m})=2.1 \times 10^{-19} \text{cm}^2$, is in close agreement with Krupke's value of $1.9 \times 10^{-19} \text{cm}^2$ (taking into account the 44 cm^{-1} splitting of level $^4F_{3/2}$).

Finally, it is useful to know that a calibrated absorption cross section spectrum around 808 nm can be found on the website of the Northrop-Grumman company [14]. It is reported there for a Nd^{3+} ion concentration of 1.6 at\% corresponding to about $2 \times 10^{20} \text{ Nd}^{3+} \text{ ions/cm}^3$, which means a maximum absorption cross section of $4.8 \times 10^{-20} \text{ cm}^2$ at about 808 nm . We report it

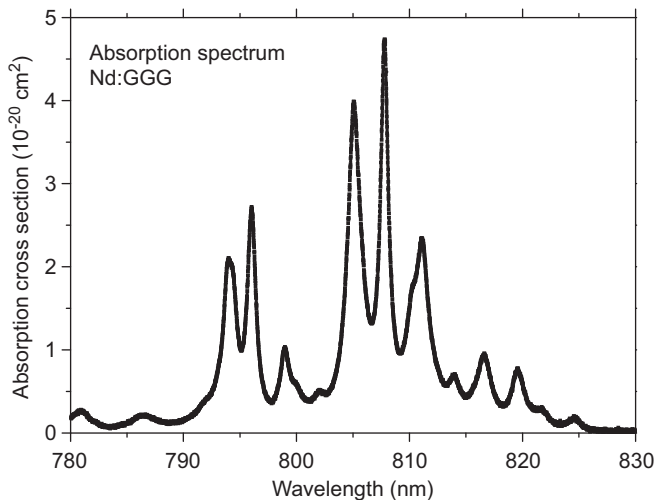


Fig. 1. Room temperature absorption cross section spectrum around 800 nm .

here again in Fig. 1, as it is registered with our own sample, for sake of clarity.

3. Experimental procedures

The absorption and emission spectra were registered by using standard commercial equipments. The emission spectra were carefully corrected for the spectral response of the apparatuses between 850 and 1450 nm in order to cover all the detectable emission transitions coming from the $^4F_{3/2}$ emitting level of the Nd^{3+} active ions down to the main terminal levels $^4I_{9/2}$, $^4I_{11/2}$ and $^4I_{13/2}$.

The absorption spectra are calibrated by using the real dopant concentration. The emission spectra are generally calibrated by using the Futchbauer–Ladenburg (FL) formula [15]:

$$\sigma_{em}^i(\lambda) = \frac{\lambda^5 \beta_i}{8 \pi c \tau_f n^2} \frac{I_i(\lambda)}{\int_i \lambda I_i(\lambda) d\lambda} \quad (1)$$

where I_i is an intensity and β_i stands for the branching ratio of the $^4F_{3/2} \rightarrow i$ th transition and can be calculated independently by writing:

$$\beta_i = \frac{\int_i \lambda I_i(\lambda) d\lambda}{\sum_{i=1,2,3} \int_i \lambda I_i(\lambda) d\lambda} \quad (2)$$

with $i=1, 2$ and 3 for the $^4F_{3/2} \rightarrow ^4I_{9/2}$, $^4F_{3/2} \rightarrow ^4I_{11/2}$ and $^4F_{3/2} \rightarrow ^4I_{13/2}$, respectively.

The excited-state absorption (ESA) spectra were registered by using a pump–probe technique [16] based on two lock-in amplifiers. The registered spectra, in fact, were ESA difference spectra which were transformed into ESA cross section spectra by determining first the excited ion density N^* at wavelengths where, according to the positions of the Nd^{3+} energy levels, there is no ESA transition (which is expected around 1.06 and $1.11 \mu\text{m}$, for instance, in the case of Nd:GGG), then by deconvoluting for the previously derived ground-state absorption and emission cross section spectra (see in Ref. [16] for more details concerning the method).

4. Emission and ESA cross section spectra

As indicated previously, the emission spectra associated with the emission transitions from the $^4F_{3/2}$ metastable level of the Nd^{3+} active ions down to the lower energy levels have been transformed into units of cross-sections by using the above reported Fuchtbauer–Ladenburg expression, the fluorescence lifetime $\tau_f=250 \mu\text{s}$, as extrapolated at zero concentration, the average Nd:GGG refractive index $n=1.94$ and the branching ratio β_i of each inter-multiplet emission transition. However, instead of using the branching ratios which can be derived from the J.O. analysis of the absorption spectra, which necessitates to be confident both on the dopant concentration and the J.O. formalism, these branching ratios were directly derived from registered emission spectra and also by reference to the case of Nd:YAG [17].

Doing so, the experimental branching ratios in the case of Nd:GGG were found equal to

$$\begin{aligned} \beta(^4F_{3/2} \rightarrow ^4I_{9/2}) &= 43.4 \pm 1.5\%, \quad \beta(^4F_{3/2} \rightarrow ^4I_{11/2}) \\ &= 47.5 \pm 1\% \quad \text{and} \quad \beta(^4F_{3/2} \rightarrow ^4I_{13/2}) \\ &= 8.8 \pm 0.7\% \end{aligned}$$

which is very close to the values reported in the past by Lomheim and De Shazer [12] by using the J.O. formalism.

The resulting emission cross section spectra are reported in Figs. 1–3. It is found the emission cross-section values

$$\sigma_{em}(937.3\text{ nm}) \approx 3 \times 10^{-20} \text{ cm}^2, \sigma_{em}(1062\text{ nm}) \approx 1.5 \times 10^{-19} \text{ cm}^2$$

and

$$\sigma_{em}(1331\text{ nm}) \approx 3.9 \times 10^{-20} \text{ cm}^2.$$

This can be compared with the values derived in the case of Nd:YAG [18], i.e.

$$\sigma_{em}(938\text{ nm}) \approx 3 \times 10^{-20} \text{ cm}^2, \sigma_{em}(1064\text{ nm}) \approx 2.7 \times 10^{-19} \text{ cm}^2$$

and

$$\sigma_{em}(1320\text{ nm}) \approx 5.2 \times 10^{-20} \text{ cm}^2.$$

The figures also show the recorded ground-(GSA) and excited-(ESA) absorption spectra in the same domains as the emission lines around 900, 1060 and 1350 nm.

It is worth noting here that the ESA spectra around 1060 and 1350 nm reported in Figs. 3 and 4 (since there is no ESA around 900 nm) have been obtained, as mentioned above, by subtracting the stimulated emission cross section spectra derived independently by calibrating the experimental emission spectra with the

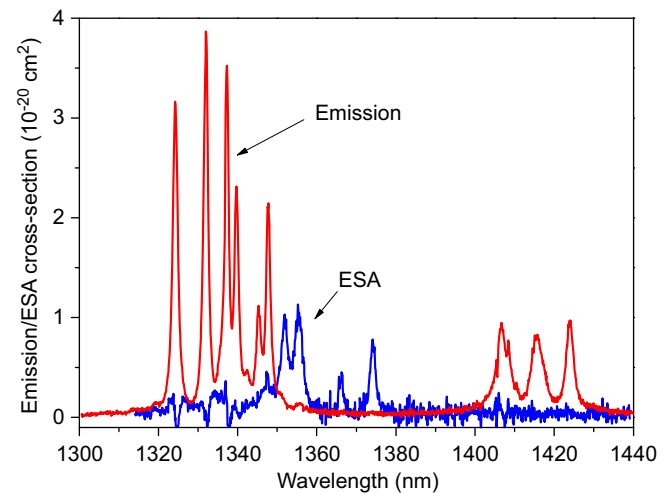


Fig. 4. Room temperature emission and excited-state absorption (ESA) cross section spectra around 1350 nm.

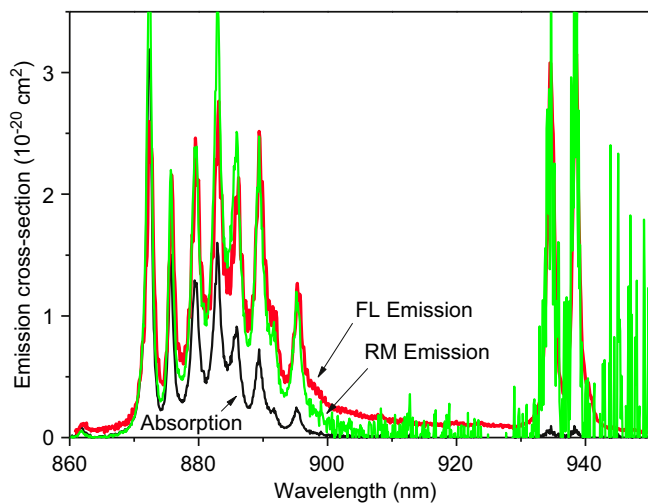


Fig. 2. Room temperature absorption and emission cross section spectra as obtained by using the Fuchbauer-Ladenburg (FL) and the Reciprocity methods (RM).

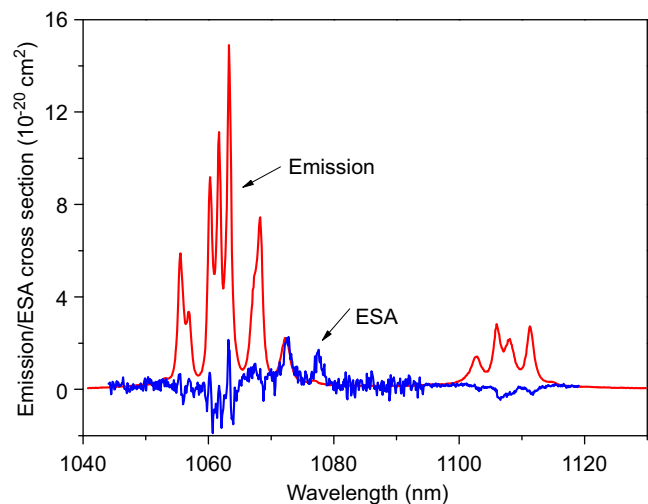


Fig. 3. Room temperature emission and excited-state absorption (ESA) cross section spectra around 1060 nm.

aid of the Fuchbauer-Ladenburg formula. It means that the reported emission cross section spectra do not depend on the quality of this deconvolution. On the contrary, the derived ESA cross section spectra may be subject to this deconvolution, for instance because of the slightly different spectral resolutions used to register the respective emission and excited-state absorption difference spectra (see in Ref. [16] for an explanation of what is really measured). Figs. 2 and 3 show that this deconvolution, indeed, is not perfect, especially around 1150 nm. Nevertheless, the deconvolution is quite good around 1060 and 1340 nm, the small and sharp negative features appearing after the deconvolution resulting from spectral resolution artefacts.

From these spectra, we can derive about the same conclusions as for the other Nd³⁺ doped laser crystals [19,20], i.e.

- no ESA around the 1062 nm emission lines.
- Nonnegligible ESA around 1330 nm (around 5%).
- No ESA around 1150 and 1410 nm.

The emission cross section values at 933.6 and 937.3 nm could be further confirmed by reconstructing the emission cross-section spectrum which can be obtained by using the so-called “reciprocity” method (RM). Indeed, the emission cross-section spectrum σ_{em} associated with the emission transition ${}^4F_{3/2} \rightarrow {}^4I_{9/2}$ can be obtained from the corresponding ${}^4I_{9/2} \rightarrow {}^4F_{3/2}$ absorption cross-section spectrum by using the expression [15]

$$\sigma_{em}(\lambda) = \sigma_{abs}(\lambda) \frac{Z_l}{Z_u} \exp \left[\frac{hc}{kT} \left(\frac{1}{\lambda_{Zl}} - \frac{1}{\lambda} \right) \right] \quad (3)$$

where Z_l and Z_u stand for the ${}^4I_{9/2}$ and ${}^4F_{3/2}$ partition functions respectively and λ_{Zl} is the wavelength of the so-called zero-line. In the case of Nd:GGG, $\lambda_{Zl}=874$ nm and, with Stark components at 0, 93, 178, 253 and 772 cm^{-1} for level ${}^4I_{9/2}$ and at 11,442 and 11,485 cm^{-1} for level ${}^4F_{3/2}$ [10,11], it is found $Z_l=4.77$ and $Z_u=3.63$, thus a ratio $Z_l/Z_u=1.32$. The corresponding spectrum (RM) is also reported in Fig. 2. It nicely fits with the spectrum obtained by using the FL expression.

Taking into account, however, the errors which can be made on one side by using the J.O. formalism and on the other side by correcting the spectra for the spectral response of the apparatuses in a spectral region where the spectral response of the detectors usually vary very strongly, we can safely estimate the emission

cross-section of the 937.3 nm emission line to

$$\sigma_{em}(937.3 \text{ nm}) = (2.95 \pm 0.1) \times 10^{-20} \text{ cm}^2$$

This is to be compared with the corresponding absorption cross-section:

$$\sigma_{abs}(937.3 \text{ nm}) = 6 \times 10^{-22} \text{ cm}^2$$

It is finally worth noting that the cross section of the other emission line at 933.6 nm, with a value of about $2.9 \times 10^{-20} \text{ cm}^2$, is only slightly lower than that at 937.3 nm. Moreover, re-absorption losses due to thermal population of the terminal level of these 3-level laser transitions should be more critical in the case of Nd:GGG, with a terminal level at about 772 cm^{-1} , than in the case of Nd:YAG, with a level at about 852 cm^{-1} . Consequently, slightly higher laser thresholds and lower output powers are expected at 933.6 nm and 937.3 nm in the case of Nd:GGG than at 946 nm and even at 938 nm in the case of Nd:YAG.

5. Conclusion

We have reported here for the first time the complete emission and excited-state absorption (ESA) cross section spectra of Nd:GGG, as registered in the near-infrared and at room temperature. As in the case of Nd:YAG, no ESA occurs at the main emission lines around 1062, 1150 and 1410 nm, but ESA does occur, although not exceeding about 5%, around the emission line at 1331 nm. Compared to Nd:YAG, it is also worth noting similar emission cross sections around 938 and 1330 nm, and an emission cross section of only half the value found in the case of Nd:YAG around 1062 nm.

Acknowledgments

This work is part of a research project entitled FLUOLASE with has been financed by the French Research Agency ANR. The

authors wish to thank the Chinese Scholarship Council (CSC) for providing the Ph.D. scholarship of Dr. Bin Xu.

References

- [1] K. Yoshida, H. Yoshida, Y. Kato, *IEEE J. Quant. Electron.* 24 (1988) 1188.
- [2] Rajni Mahajan, A.L. Shah, Suranjan Pal, Anil Kumar, *Opt. Laser Technol.* 39 (2007) 1406.
- [3] L.J. Qin, D.Y. Tang, G.Q. Xie, C.M. Dong, Z.T. Jia, X.T. Tao, *Laser Phys. Lett.* 5 (2008) 100.
- [4] Z. Jia, X. Tao, C. Dong, X. Cheng, W. Zhang, F. Xu, M. Jiang, *J. Cryst. Growth* 292 (2) (2006) 386.
- [5] A. Richter, E. Heumann, G. Huber, V. Ostroumov, W. Seelert, *Opt. Express* 15 (2007) 5172.
- [6] F. Cornacchia, A. Di Lieto, M. Tonelli, A. Richter, E. Heumann, G. Huber, *Opt. Express* 16 (2008) 15932.
- [7] B. Xu, P. Camy, J.L. Doualan, Z. Cai, R. Moncorgé, *Opt. Express* 19 (2) (2011) 1191.
- [8] J.E. Geusic, H.M. Marcos, L.G. Van Uitert, *Appl. Phys. Lett.* 4 (1964) 182.
- [9] W.F. Krupke, *Opt. Commun.* 12 (2) (1974) 210.
- [10] A.A. Kaminskii, V.V. Osiko, S.E. Sarkisov, M.I. Timochchkin, E.V. Zharikov, J. Bohm, P. Reiche, D. Schultze, *Phys. Status Solidi A* 49 (1978) 305.
- [11] A.A. Kaminskii, *Crystalline Lasers: Physical Processes and Operating Schemes*, CRC Press, Inc., 1996, p. 149.
- [12] T.S. Lomheim, L.G. De Shazer, *Phys. Rev. B* 20 (10) (1979) 4343.
- [13] M.D. Rotter, B. Dane, *Opt. Commun.* 198 (2001) 155.
- [14] <http://www.as.northropgrumman.com/products/synoptics_nd_ggg/index.html>.
- [15] S.A. Payne, L.L. Chase, L.K. Smith, W.L. Kway, W.F. Krupke, *IEEE J. Quant. Electron.* 28 (1992) 2619.
- [16] P. Le Boulanger, J.L. Doualan, S. Girard, J. Margerie, R. Moncorgé, *Phys. Rev. B* 60 (16) (1999) 11380.
- [17] G.W. Burdick, C.K. Jayasankar, F.S. Richardson, *Phys. Rev. B* 50 (1994) 16309.
- [18] R. Moncorgé, B. Chambon, J.Y. Rivoire, N. Garnier, E. Descroix, P. Laporte, H. Guillet, S. Roy, J. Mareschal, D. Pelenc, J. Doury, P. Farge, *Opt. Mater.* 8 (1997) 109.
- [19] Y. Guyot, R. Moncorgé, *J. Appl. Phys.* 73 (1993) 8526.
- [20] Y. Guyot, H. Manaa, J.Y. Rivoire, R. Moncorgé, N. Garnier, E. Descroix, M. Bon, P. Laporte, *Phys. Rev. B* 51 (1995) 784.